ELSEVIER

Journal of Alloys and Compounds 459 (2008) 395–398

Journal of ALLOYS AND COMPOUNDS

www.elsevier.com/locate/jallcom

# A facile synthesis and photoluminescence of porous S-doped ZnO architectures

Zhenwei Tao, Xibin Yu *, Jie Liu, Liangzhun Yang, Shiping Yang

*Department of Chemistry, Shanghai Normal University, Shanghai 200234, PR China*

Received 3 March 2007; received in revised form 15 April 2007; accepted 21 April 2007
Available online 4 May 2007

**Abstract**

A facile process is demonstrated to synthesize porous S-doped ZnO architectures. The products were characterized by X-ray diffraction (XRD), Raman spectrum, scanning electron microscopy (SEM), energy-dispersive X-ray spectroscopy (EDX), and photoluminescence (PL) spectra, respectively. The results indicate that the porous structured products are composed of many pores and wormlike nanoparticles with sizes ranging from 100 to 300 nm, exhibiting a strong green emission and a relatively weak ultraviolet emission. The correlation between structure and photoluminescence is also discussed.


*Keywords:* Phosphors; Luminescence

## 1. Introduction

In recent years, one of the significant goals of materials scientists has been tailoring the structure to obtain special morphologies for the design and development of new materials for more and more advanced applications [1–5]. It is well-known that the shape and size of inorganic functional materials have an important influence on their electrical and optical properties [6,7]. Control of structure with different ways is therefore the key in achieving viable applications in various fields. However, until now, it still remains a great challenge to develop simple and facile methods for fabricating those particular structures.

As an n-type semiconductive material, zinc oxide (ZnO) has received a considerable amount of attention over the past few years resulting from its many potential practical applications, such as piezoelectric transducers, optical waveguides, surface acoustic wave devices, varistors, phosphors, transparent conductive oxides, chemical and gas sensors, spin functional devices, and UV-light emitters [8,9]. ZnO is a promising material for photonic applications in UV or blue spectral range due to its wide bandgap (3.37 eV at room temperature), while the large exciton-binding energy (60 mV) makes efficient excitonic emission even at room temperature. In addition, ZnO is biocompatible material and can be directly used for biomedical applications [10].

Currently, modification of ZnO properties by chemical doping has become a hot topic, as the incorporated elements offers an effective method to adjust its electrical, optical, and magnetic properties, which is important for its practical application [11,12]. More and more attention has been paid to chalcogen elements doping in ZnO, as S-doping in ZnO is expected to modify the electrical and optical properties between S and O. S-doped ZnO films and one-dimensional (1D) nanostructures such as nanowires and nanonails have been synthesized successfully by various methods [13–17]. However, the preparation methods mentioned above involve complex procedures, sophisticated equipment and rigorous experimental conditions. Furthermore, to the best of our knowledge, studies on S-doped ZnO microstructures are rarely reported. In the present paper, we demonstrate a simple, direct and reproducible synthetic method for preparing porous S-doped ZnO architectures by a direct air oxidation process. The as-obtained products present good photoluminescent properties. The correlation between the structure and photoluminescence is also discussed.

## 2. Experimental

In a typical synthesis, 1.0 g of ZnS powders (99.99%, Shanghai Chemical) were placed in a crucible and transferred into the furnace preheated to 700 °C.

* Corresponding author. Tel.: +86 21 64324528.
*E-mail addresses:* xibinyu@shnu.edu.cn, luminescence2006@126.com (X. Yu).

0925-8388/$ – see front matter © 2007 Elsevier B.V. All rights reserved.
doi:10.1016/j.jallcom.2007.04.273

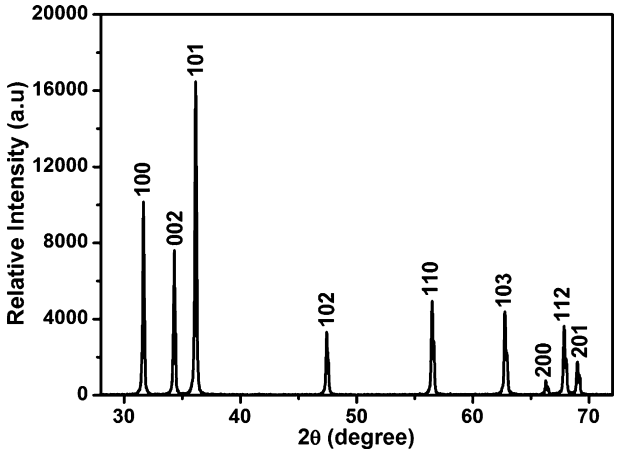


Fig. 1. XRD pattern of porous S-doped ZnO architectures.

The porous S-doped ZnO architectures were obtained by annealing the above ZnS powders in air for 60 min.

X-ray diffraction (XRD) patterns were carried out on a Rigaku D/MAX 2000 diffractometer equipped with Cu/Kα radiation (λ = 0.15405 nm) (40 kV, 40 mA). The Raman spectra were recorded on a confocal laser micro-Raman spectrometer (JY Super Ram II). The morphologies of as-obtained products were examined by scanning electron microscopy (SEM, JEOL, JSM-6460). The composition of the porous structured products was detected by energy-dispersive X-ray spectroscopy (EDX, EDAX, Genesis). The photoluminescence (PL) spectra were taken on a Cary-Eclipse 500 spectrofluorometer (VARIAN) with a 60 W Xenon lamp as excitation source.

## 3. Results and discussion

The porous structured S-doped ZnO products were structurally characterized by X-ray diffraction (XRD). A typical XRD pattern is shown in Fig. 1. It can be seen that all of these peaks are in good agreement with wurtzite ZnO (JCPDS Card, No. 36-1451). The strong and clear peaks indicate the high purity and crystallinity of the as-obtained products. No characteristic peaks were observed for other impurities such as ZnS. Fig. 2 shows the Raman spectrum of as-obtained products. An intense peak at 441 $cm^{-1}$ is observed which match the corresponding nonpolar optical phonon $E_2$ mode [18]. No peaks from ZnS or other impurities were detected. The results of XRD and Raman spectrum indicate that the existent S may have occupied the O sites.

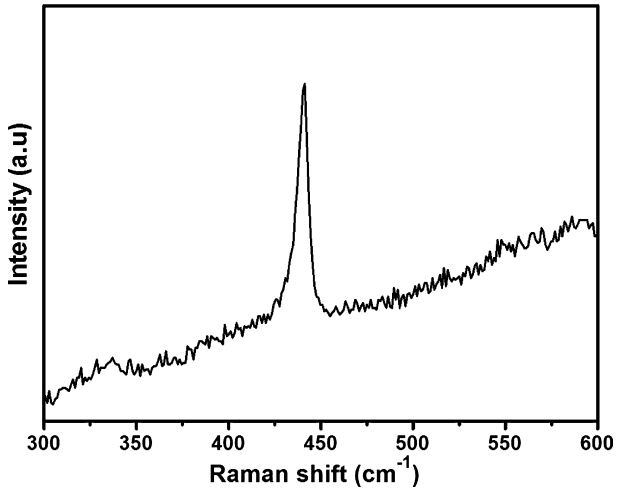


Fig. 2. Raman spectrum of porous S-doped ZnO architectures.

The morphology of porous structured S-doped ZnO products was investigated by scanning electron microscopy (SEM), as shown in Fig. 3a. It shows that the as-obtained products are composed of near spherical particles with the average size in the range of 3–4 μm. Careful observation indicates that the surface of these particles is much rougher than that of initial ZnS particles (see Fig. S1 in Supporting Information). Simultaneously, many pores and wormlike nanoparticles with sizes ranging from 100 to 300 nm can be seen clearly on the surface. It seems that the big particles are constructed by lots of these small nanoparticles.

To investigate the formation mechanism of the porous structured S-doped ZnO products, same ZnS powders were annealed at the identical condition for 30 and 120 min, and the morphologies of as-obtained particles are shown in Fig. 3 b and c, respectively. It can be seen that the surface of particles annealed for 30 min has become a bit accidented. The profile of the wormlike nanoparticles is already discernable, while only a few pores can be observed (Fig. 3b). However, when particles were annealed for 120 min, the surface becomes much smoother than that annealed for 60 min, whereas those wormlike nanoparticles have been agglomerated into bigger ones and nearly no pores can be found on the surface (Fig. 3c). In the annealing process, the surface of ZnS particles was etched by oxygen contained in air, and then wormlike nanoparticles were formed gradually on the particles surface. At the same time, gases like $SO_2$, etc. were produced as ZnS was oxidized into ZnO. Consequently, pores were easily formed due to the release of these gases. As annealing time increased, the amount of ZnS decreased continuously and fewer gases were produced. Those pores formed before would be eliminated gradually owing to the improvement of the structure at the high annealing temperature. The surface area of the porous S-doped ZnO architectures is 20.81 $m^2\ g^{-1}$, while the value of the initial ZnS powders is only 8.51 $m^2\ g^{-1}$. The composition of the porous structured products is identified by energy-dispersive X-ray spectroscopy (EDX). The EDX pattern is displayed in Fig. 3d. It indicates that the as-obtained products are composed of Zn, O, and a small quantity of S. The S content is 2.8 at.% measured by EDX.

PL spectra are powerful tools which are used widely to investigate the effect on luminescent properties of ZnO from S doping, as described in many previous reports [14–17]. Fig. 4a shows the PL spectrum of the porous S-doped ZnO architectures annealed for 60 min. Two luminescence bands are observed in the visible region under 340 nm UV excitation. One is a relative weak and narrow UV emission peaking at about 393 nm corresponds to the near band edge (NBE) emission, which is responsible for the recombination of the free excitons of ZnO [19]. Another is a strong and broad green emission band centered at 496 nm, which may originate from the commonly assumed the recombination of the photoexcited holes with the electrons occupying the singly ionized oxygen vacancies [20,21]. The PL spectra of as-obtained products annealed for 30 and 120 min are also presented in Fig. 4b and c, respectively. It can be seen that the products annealed for 30 min as well as the special struc-

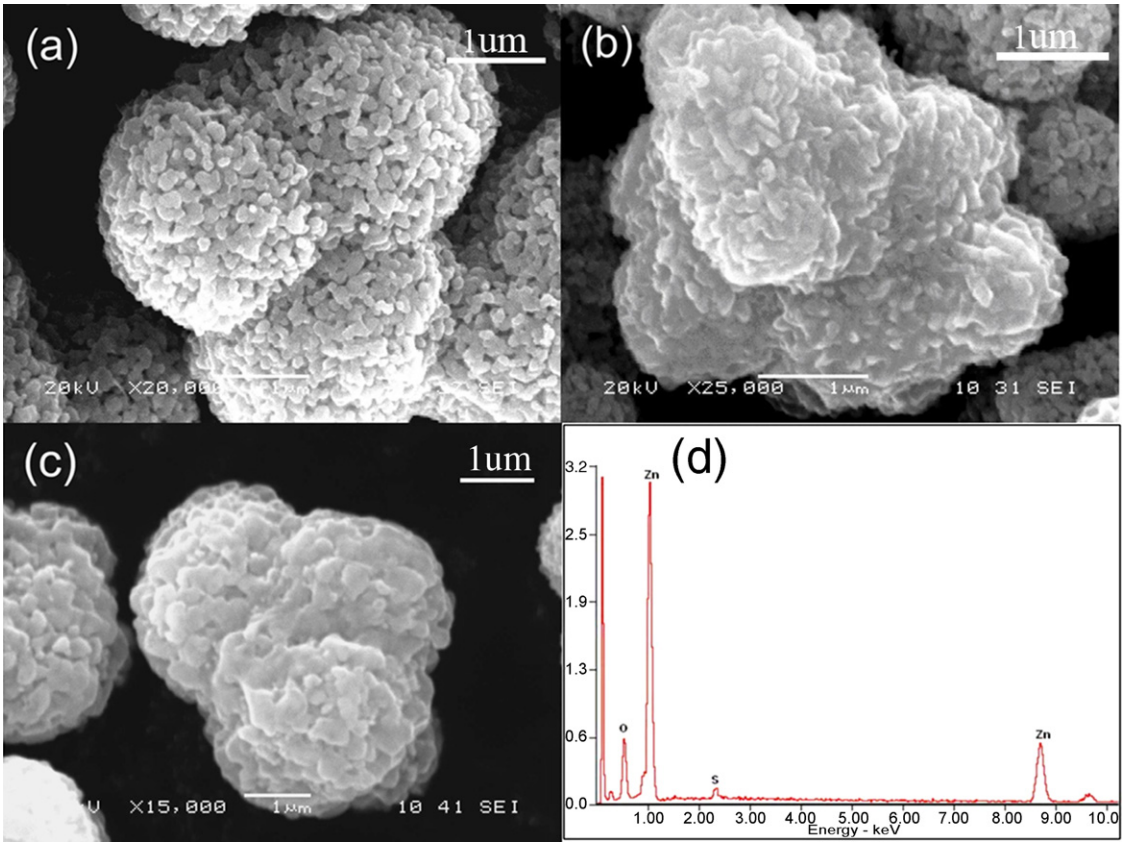


Fig. 3. (a) SEM images of the porous S-doped ZnO architectures. (b and c) SEM images of as-obtained particles annealed for 30 and 120 min, respectively. (d) EDX spectrum of the porous S-doped ZnO architectures.

tures possess a much stronger green emission band than the NBE band, while the products annealed for 120 min show the contrary behavior. In addition, no noticeable shift in the NBE emission band is observed, except some broadening in the band for the products annealed for 120 min. It is believed that the green emission is related to the oxygen defects closely, since S has a larger Bohr radius than O, the incorporation of S into the ZnO crystal lattice introduces lattice distortion inevitably. This influences the energy structure of ZnO and gives rise to some new defects, especially oxygen vacancies, which leads to the remarkable enhancement of the green emission band. From the PL spectra, it can be seen that the intensity of the green emission for porous S-doped ZnO architectures is much stronger than the other two products. The influences from the incorporated S are necessary. However, here, the effect of the structure on the PL intensity of the green emission should be regarded. Djurišić et al. [22] proposed that the green emission might originate from surface defects. According to the SEM analysis, the porous structured products show a much rougher surface compared with the other two products. It is reasonable to believe that the density of the defects located on the particles surface is much higher for the porous S-doped ZnO architectures, which induces the increase in the PL intensity of green light emission. Moreover, it has also been proposed that the green emission of ZnO nanowires increases with the surface to volume ratio increases [23]. Thus the as-prepared architectures will also exhibit much intense green emission due to the larger surface area.

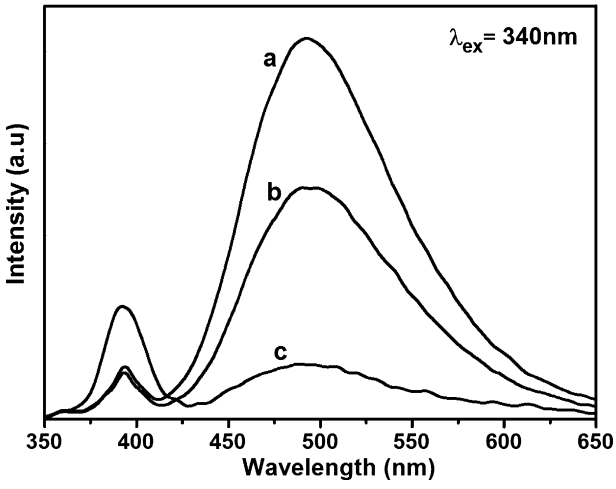


Fig. 4. PL spectra of porous S-doped ZnO architectures (a), and as-obtained products annealed for 30 min (b) and 120 min (c).

## 4. Conclusions

In summary, a facile approach has been explored to synthesize porous S-doped ZnO architectures. The as-obtained products are composed of many pores and wormlike nanoparticles with sizes ranging from 100 to 300 nm. The PL spectra of as-obtained porous structures consist of a relatively weak ultraviolet emis-

sion band peaking around 393 nm and a broad and strong green emission band centered at 496 nm. A possible mechanism has also been proposed, which presents the possibility of synthesizing other porous structured composites.

## Acknowledgements

This work was supported by Science and Technology Development Fund, Shanghai, China, Project No. 04JC14089. 0452nm070 and Shanghai Leading Academic Discipline Project, Project Number: T0402.

## Appendix A. Supplementary data

Supplementary data associated with this article can be found, in the online version, at doi:10.1016/j.jallcom.2007.04.273.

## References

[1] P.X. Gao, Y. Ding, W. Mai, W.L. Hughes, C. Lao, Z.L. Wang, Science 309 (2005) 1700.
[2] H. Deng, X. Li, Q. Peng, X. Wang, J. Chen, Y. Li, Angew. Chem. Int. Ed. 18 (2005) 2782.
[3] C. Yan, D. Xue, J. Phys. Chem. B 109 (2005) 12358.
[4] C. Yan, D. Xue, L. Zou, X. Yan, W. Wang, J. Cryst. Growth 282 (2005) 448.
[5] U.K. Gautam, S.R.C. Vivekchand, A. Govindaraj, G.U. Kulkami, N.R. Selvi, C.N.R. Rao, J. Am. Chem. Soc. 127 (2005) 3658.
[6] A.P. Alivisatos, Science 271 (1996) 933.
[7] Y. Zhang, Y.D. Li, J. Phys. Chem. B 108 (2004) 17805.
[8] Ü. Özgür, Ya.I. Alivov, C. Liu, A. Teke, M.A. Reshchikov, S. Doğan, V. Avrutin, S.-J. Cho, H. Morkoç, J. Appl. Phys. 98 (2005) 041301.
[9] R. Triboulet, J. Perriere, Prog. Cryst. Growth Charact. Mater. 47 (2003) 65.
[10] R. Yaparpalvi, S.K. Loyalka, R.V. Tompson, J. Biomed. Mater. 28 (1994) 1087.
[11] X. Duan, Y. Huang, Y. Cui, C.M. Lieber, Nature 409 (2001) 66.
[12] Y.H. Tang, T.K. Sham, A. Jurgensen, Y.F. Hu, C.S. Lee, S.T. Lee, Appl. Phys. Lett. 80 (2002) 3709.
[13] Y.-Z. Yoo, W.J. Zheng, T. Chikyow, T. Fukumura, M. Kawasaki, H. Koinuma, Appl. Phys. Lett. 81 (2002) 3798.
[14] Y.B. Geng, G.Z. Wang, Z. Jiang, T. Xie, S.H. Sun, G.W. Meng, L.D. Zhang, Appl. Phys. Lett. 82 (2003) 4791.
[15] S.Y. Bae, H.W. Seo, J. Park, J. Phys. Chem. B 108 (2004) 5206.
[16] G.Z. Shen, J.H. Cho, J.K. Yoo, G.-C. Yi, C.J. Lee, J. Phys. Chem. B 109 (2005) 5491.
[17] G.Z. Shen, J.H. Cho, S.I. Jung, C.J. Lee, Chem. Phys. Lett. 401 (2005) 529.
[18] T.C. Damen, S.P.S. Porto, B. Tell, Phys. Rev. 142 (1966) 570.
[19] Y.C. Kong, D.P. Yu, B. Zhang, W. Fang, S.Q. Feng, Appl. Phys. Lett. 78 (2001) 407.
[20] K. Vanheusden, W.L. Warren, C.H. Seager, D.R. Tallant, J.A. Voigt, B.E. Gnade, J. Appl. Phys. 79 (1996) 7983.
[21] K. Vanheusden, C.H. Seager, W.L. Warren, D.R. Tallant, J.A. Voigt, Appl. Phys. Lett. 68 (1996) 403.
[22] A.B. Djurišić, W.C.H. Choy, V.A.L. Roy, Y.H. Leung, C.Y. Kwong, K.W. Cheah, T.K.G. Rao, W.K. Chan, H.F. Lui, C. Surya, Adv. Funct. Mater. 14 (2004) 856.
[23] M.H. Huang, Y. Wu, H. Feick, N. Tran, E. Weber, P. Yang, Adv. Mater. 13 (2001) 113.